

# Thermal diffusivity and heat capacity of poly(vinylidene fluoride)/poly(methyl methacrylate) blends by flash radiometry

Naoto Tsutsumi\*, Masaru Terao and Tsuyoshi Kiyotsukuri

Department of Polymer Science and Engineering, Kyoto Institute of Technology,  
Matsugasaki, Sakyo, Kyoto 606, Japan

(Received 19 November 1991; revised 27 February 1992)

The thermal diffusivity  $D$  and the relative heat capacity  $HC$  were measured for poly(vinylidene fluoride)/poly(methyl methacrylate) (PVDF/PMMA) blends by flash radiometry. The effect of the crystal form on  $D$  of these polymer blends as well as the dependence of  $D$  and  $HC$  on temperature were discussed. In the PVDF content region between 70 and 80 wt%, the blend samples preferentially form the  $\beta$  crystal phase when they are prepared by melt quenching. The dependence of  $D$  on PVDF content for the melt-quenched sample showed a noticeable change in the composition region in which the  $\beta$  crystal phase is formed.  $D$  decreased with increasing PVDF content up to 70 wt% and then increased up to 100 wt%, showing a peak between 75 and 80 wt%. From the X-ray diffraction patterns, the crystallinity of the blends monotonically decreases with decrease of PVDF content. The results imply that the peak in  $D$  in the melt-quenched 75/25 and 80/20 PVDF/PMMA blends is not related to the crystallinity but to another structural factor. The temperature profile of  $D$  showed inflection points corresponding to the glass transition temperature and the melting temperature of the  $\alpha$  crystal phase. The temperature profile of  $HC$  exhibited changes of  $HC$  due to the melting transition of the  $\beta$  and  $\alpha$  crystal phases. These points from the temperature profile of  $D$  and  $HC$  correspond well to those from thermal analysis.

(Keywords: thermal properties; thermal diffusivity; heat capacity; blends; poly(vinylidene fluoride); poly(methyl methacrylate); flash radiometry)

## INTRODUCTION

A new technique for measuring the thermal diffusivity of solid materials, flash radiometry (pulsed photothermal radiometry), has been reported by us<sup>1-4</sup> and by other researchers<sup>5-8</sup>. We have suggested flash radiometry as a useful tool to estimate the supermolecular structure of polymer solids<sup>2,3</sup>.

Polymer blends are important materials for improving chemical, physical and mechanical properties. However, there are few reports on the thermal diffusion and conduction properties of polymer blends, in spite of the fact that they include the important properties of mass transfer at the interface.

Poly(vinylidene fluoride) (PVDF) and poly(methyl methacrylate) (PMMA) blends are compatible in all blend proportions in the molten state<sup>9</sup>. The FT-i.r. study of PVDF/PMMA has shown that the 70/30 blend (by weight) leads directly to the  $\beta$  crystal form of PVDF when the blend is quenched from the melt and then annealed at higher temperature<sup>10</sup>. A separate study of the PVDF/PMMA blend revealed that a melt-quenched sample of 80 wt% PVDF and 20 wt% PMMA also preferentially forms the  $\beta$  crystal form (type I) and this crystallite increases in size when the sample is annealed at higher temperature<sup>11</sup>.

We have measured the thermal diffusivity and the relative heat capacity of these PVDF/PMMA blends with various blend ratios, and found that the melt-quenched PVDF/PMMA sample had a significant peak in thermal diffusivity at a blend ratio of 80/20 and 75/25. In this study, we report the measurement of the thermal diffusivity and the relative heat capacity of these PVDF/PMMA blends and discuss the effect of crystal form on the thermal diffusivity of these polymer blends as well as the temperature dependences of thermal diffusivity and heat capacity.

## EXPERIMENTAL

### Sample preparation

PVDF (Kureha, KF-polymer,  $M_w = 141\ 000$ ,  $M_n = 64\ 000$ ) and PMMA (Mitsubishi Rayon, Acrypett-VHK,  $M_w = 168\ 000$ ,  $M_n = 96\ 400$ ) were used. The polymers were mechanically melt blended at 200°C and were then melt pressed between 50  $\mu\text{m}$  thick films of Upilex (Ube Industry, Japan) on a heated press to a thickness between 50 and 100  $\mu\text{m}$ . The molten films were quenched in liquid nitrogen or slowly cooled in a hot press at a rate of ca. 1°C min<sup>-1</sup>.

### Flash radiometry

The thermal diffusivity  $D$  and the relative heat capacity  $HC$  of the blend films were measured by flash radiometry.

\*To whom correspondence should be addressed

Carbon layers of ca. 1  $\mu\text{m}$  thickness were coated onto both surfaces of the blend films. When the rear surface of the coated film was heated by a light pulse, the transient heat transport in the sample film was observed by the infra-red radiation from the front carbon layer on the film. The transient infra-red signal  $S(t)$  was detected by an HgCdTe infra-red detector (Fujitsu model MC-A), digitized and stored in a microcomputer for data analysis.  $D$  and  $HC$  were independently determined by simulating the obtained transient signal  $S(t)$  by the following theoretical curve for one-dimensional heat diffusion, using a non-linear least-squares method:

$$S(t) = (KQ/CL) \left( 1 + 2 \sum_{n=1}^{\infty} (-1)^n \exp(-n^2 \pi^2 Dt/L^2) \right) \quad (1)$$

Here  $K$  ( $= 4G\epsilon\sigma T_0^3$ ) is a constant including a geometrical factor  $G$ , emissivity  $\epsilon$ , Stefan-Boltzmann constant  $\sigma$  and temperature  $T_0$  of the sample before pulse heating;  $Q$  is the total thermal energy absorbed by the carbon layer;  $C$  is the heat capacity of the sample; and  $L$  is the sample thickness. After simulating the signal, optimum values of  $D$  and  $\Delta T$  ( $= KQ/CL = K'QT_0^3/CL$ , where  $K' = 4G\epsilon\sigma$ ) were determined, and then the relative capacity  $HC$  ( $= C/K'Q = T_0^3/\Delta TL$ ) was computed. The detailed procedure for the measurement and calculation of  $D$  and  $\Delta T$  has been described in our previous papers<sup>1,3</sup>.

#### Characterization

X-ray diffraction patterns were measured with a Toshiba model ADG-301 X-ray diffractometer with nickel-filtered  $\text{Cu K}\alpha$  radiation. Differential thermal analysis (d.t.a.) was carried out in a nitrogen atmosphere on a Shimadzu model DT-30 differential thermal analyser at a heating rate of  $10^\circ\text{C min}^{-1}$ , except where otherwise specified in the text. Thermomechanical analysis (t.m.a.) was performed in penetration mode under a pressure of  $10 \text{ kg cm}^{-2}$  and a heating rate of  $10^\circ\text{C min}^{-1}$  in a nitrogen atmosphere, using a Seiko Instruments model TMA100 thermomechanical analyser and recorded on a model SSC5200H disk station for data analysis.

## RESULTS AND DISCUSSION

#### Dependence of $D$ on blend composition

The X-ray diffraction patterns in *Figure 1* show that the melt-quenched 80/20 and 70/30 PVDF/PMMA blends have diffraction peaks characteristic of the  $\beta$  crystal phase of PVDF at  $20.8$  and  $41.2^\circ$ , whereas 85/15 PVDF/PMMA blend and pure PVDF exhibit peaks at  $17.6$ ,  $18.4$ ,  $20.0$ ,  $26.6$  and  $38.7^\circ$  due to the  $\alpha$  crystal phase of PVDF. These angles are shown by arrows in the figure. The intensity of these characteristic peaks due to the  $\beta$  crystal phase increased when the sample film was annealed at higher temperature. The 75/25 PVDF/PMMA blend also showed the formation of the  $\beta$  crystal phase when the sample was prepared by melt quenching.

*Figure 2* shows the dependence of  $D$  on the blend ratio for the blend samples prepared by melt quenching and slow cooling. All  $D$  values were measured at room temperature. For a PVDF content below 70 wt%,  $D$  of the melt-quenched sample monotonically decreases with increasing PVDF content, which is explained by the decrease of PMMA component having higher thermal

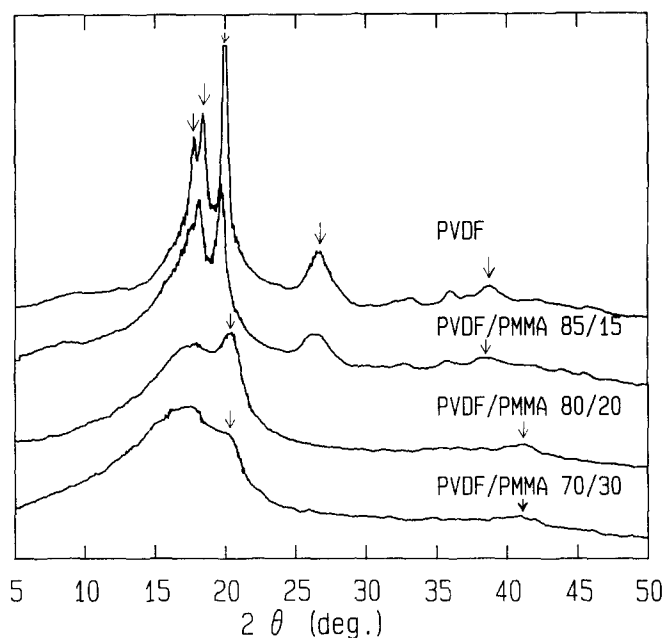


**Figure 1** X-ray diffraction patterns of the melt-quenched samples

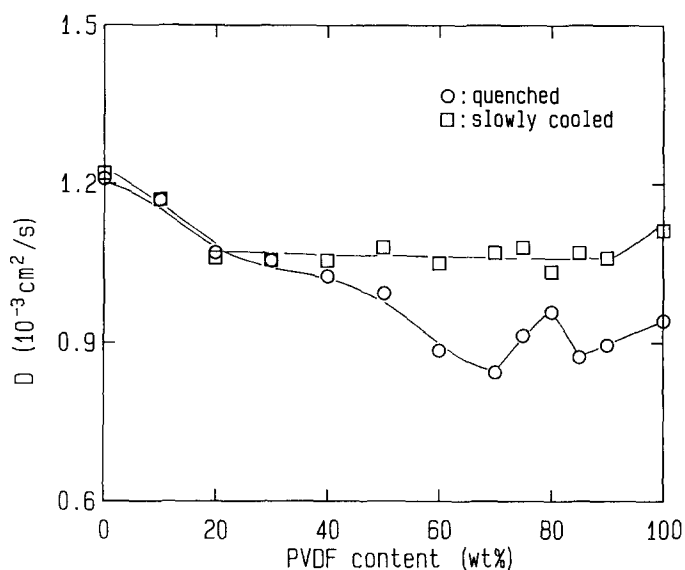


**Figure 2** Plots of  $D$  versus PVDF content for the samples provided by melt quenching and slow cooling

diffusivity. For a PVDF content above 70 wt%,  $D$  increases with PVDF content, corresponding to the increase of crystallinity of the PVDF component as estimated from the X-ray diffraction patterns in *Figure 1*. However, the melt-quenched samples with 75 and 80 wt% PVDF contents, at which the  $\beta$  crystal phase is formed, have anomalously larger  $D$  values than those expected from their relatively lower crystallinity. Therefore, the large  $D$  of the melt-quenched 75/25 and 80/20 PVDF/PMMA blends is not related to the crystallinity. We have previously reported<sup>3</sup> that a difference in the type of growth of poly(ethylene terephthalate) (PET) crystallites on isothermal crystallization might affect the aggregation state of the amorphous region of PET, and thus result in the specific increase of  $D$ . There has been other discussion on the comparison of the thermal diffusivity between miscible and immiscible blends. It was reported that the thermal diffusivity of immiscible PMMA/poly(vinyl chloride)

(PVC) is larger than that of miscible PMMA/PVC<sup>12</sup>. We do not have a definite interpretation for the large  $D$  of the melt-quenched 75/25 and 80/20 PVDF/PMMA blends, but we can say that it may imply phase separation in the amorphous region of these blends or the fact that the  $\beta$  crystal phase affects the aggregation state of the amorphous region of these blends.

The slowly cooled samples above a PVDF content of 30 wt% have almost the same  $D$  except for the fact that pure PVDF has a slightly larger  $D$ . The X-ray diffraction pattern showed that the slowly cooled samples exhibited the  $\alpha$  crystal phase above a PVDF content of 50 wt%. The growth of spherulites in the slowly cooled samples of PVDF content above 50 wt% was confirmed under a polarized microscope. The shape of the spherulite of pure PVDF was clear and the size of the spherulite of pure PVDF was larger than that of other blend samples. The difference of spherulite size may be related to a slight difference in  $D$  between pure PVDF and other blend samples.

Temperature dependence of  $D$

The temperature dependence of  $D$  of the melt-quenched samples can be divided into three groups depending on the shape of the profile: samples from PVDF/PMMA (100/0) to (70/30) have almost the same profile, which is designated as group A; samples of (60/40) and (50/50) are group B; and samples from (40/60) to (0/100) are group C. Typical temperature profiles of  $D$  for each group are shown in Figure 3, in which the significant inflection points are shown by arrows. The temperature profile of  $D$  of the 90/10 PVDF/PMMA blend in group A has a maximum in the vicinity of 171°C, which corresponds to melting of the  $\alpha$  crystal phase at 172°C in the d.t.a. curve. The 50/50 PVDF/PMMA blend in group B has three inflection points at 50, 93 and 166°C in the temperature profile of  $D$ . T.m.a. data showed that the 50/50 PVDF/PMMA sample had a heat distortion temperature at 57°C corresponding to the glass transition, and the d.t.a. data exhibited an endothermic peak at 162°C due to melting of the  $\alpha$  crystal phase. Thus the inflection points at 50 and 166°C correspond to the glass transition temperature  $T_g$  and the melting temperature  $T_m$ , respectively. In the temperature range above 93°C,  $D$

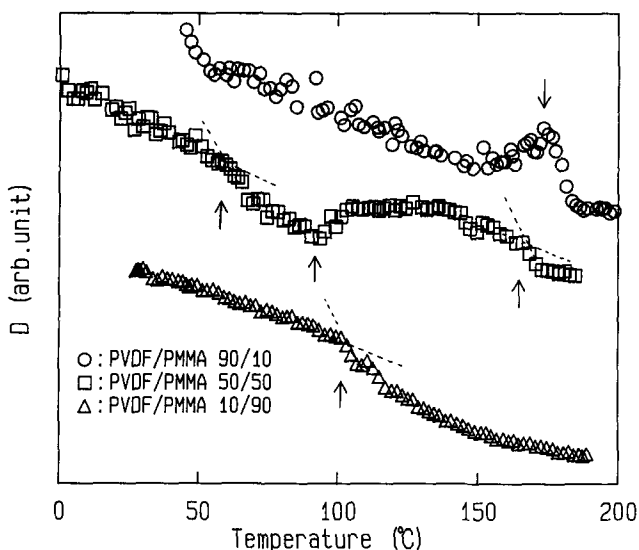


Figure 3 Typical examples of temperature dependence of  $D$  for blends

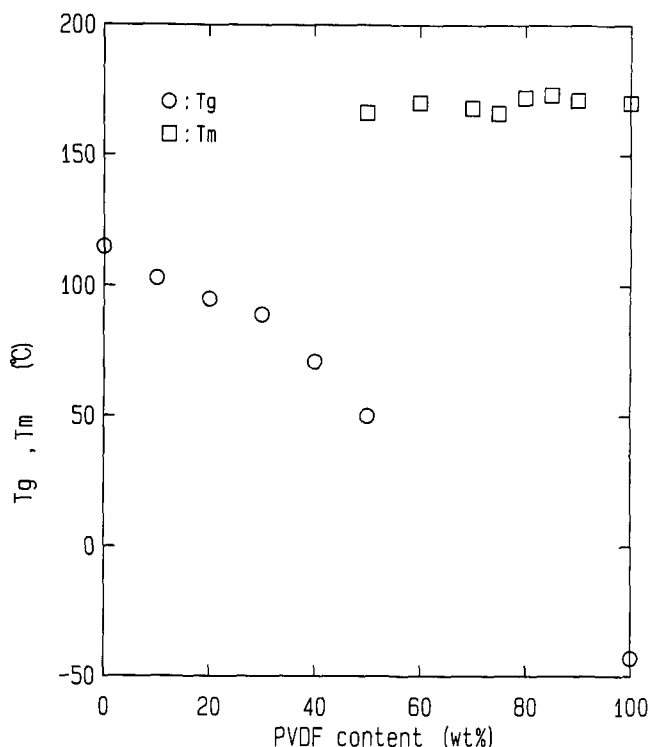


Figure 4 Plots of  $T_m$  and  $T_g$  by flash radiometry versus the PVDF content

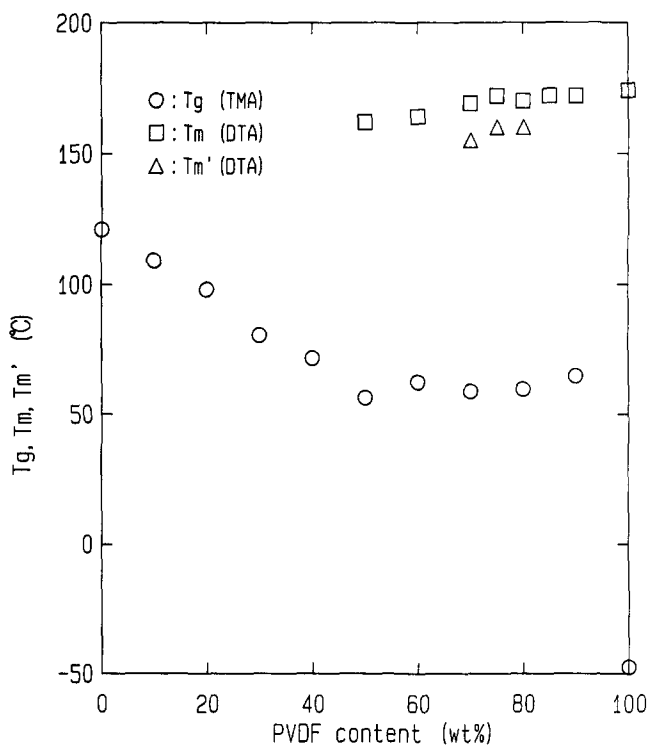


Figure 5 Plots of  $T_m$  and  $T_g$  by thermal analysis versus the PVDF content

increases, which will be discussed later. The 10/90 PVDF/PMMA blend in group C has an inflection point at 103°C, which corresponds to  $T_g$ . The melting temperature  $T_m$  and the glass transition temperature  $T_g$  by flash radiometry are plotted against the PVDF content in Figure 4. Plots of  $T_m$  by d.t.a. and  $T_g$  by t.m.a. are shown in Figure 5. Both  $T_m$  and  $T_g$  in Figure 4 correspond well to  $T_m$  and  $T_g$  in Figure 5 for each PVDF content, respectively. In the d.t.a. curves of 80/20, 75/25 and

70/30 PVDF/PMMA blends, there was another distinct endothermic peak in the vicinity of  $160^{\circ}\text{C}$ , which is just below  $T_m$ . These points are indicated as  $T'_m$  (open triangles) in Figure 5. When decreasing the heating rate of d.t.a. measurement of the melt-quenched PVDF/PMMA (80/20), a significant exothermic peak appeared between  $T'_m$  and  $T_m$ , and a slower heating rate causes a more distinct exothermic peak, as shown by an arrow in Figure 6. D.t.a. remeasurement was carried out for samples that were heated up in advance to (a)  $157^{\circ}\text{C}$ , (b)  $163^{\circ}\text{C}$  and (c)  $167^{\circ}\text{C}$  at a heating rate of  $10^{\circ}\text{C min}^{-1}$  in the d.t.a. cell and then melt-quenched. The result is shown in Figure 7. The increase of the heated-up temperature gave rise to a decrease of intensity of the lower peak and an increase of intensity of the higher peak. Further, the X-ray diffraction pattern of the 80/20 PVDF/PMMA blend annealed at  $160^{\circ}\text{C}$  and then melt-quenched gave rise to the formation and growth of the  $\alpha$  crystal phase, and more prolonged annealing resulted in more  $\alpha$  crystal growth. These results imply that the  $\beta$  crystal melts at  $T'_m$  (ref. 13) and successive recrystallization above  $T'_m$  occurs to form the  $\alpha$  crystal phase, which melts at  $T_m$ . In the temperature profile of  $D$ , points related to  $T'_m$  for the 80/20, 75/25 and 70/30 PVDF/PMMA blends could not be observed.

The temperature profile of  $D$  of group B exhibits an increment of  $D$  above  $93^{\circ}\text{C}$ , which was already shown in Figure 3. When decreasing the heating rate, this inflection point lowers as shown by the arrow in Figure 8 ( $93$ ,  $88$  and  $76^{\circ}\text{C}$  at  $1$ ,  $0.6$  and  $0.2^{\circ}\text{C min}^{-1}$ , respectively), whereas the inflection points due to the glass transition temperature and the melting temperature are not changed by the heating rate but are almost constant in the vicinity of  $50^{\circ}\text{C}$  and  $166^{\circ}\text{C}$ , respectively. D.t.a. measurement of this blend at a heating rate of  $1^{\circ}\text{C min}^{-1}$  showed the

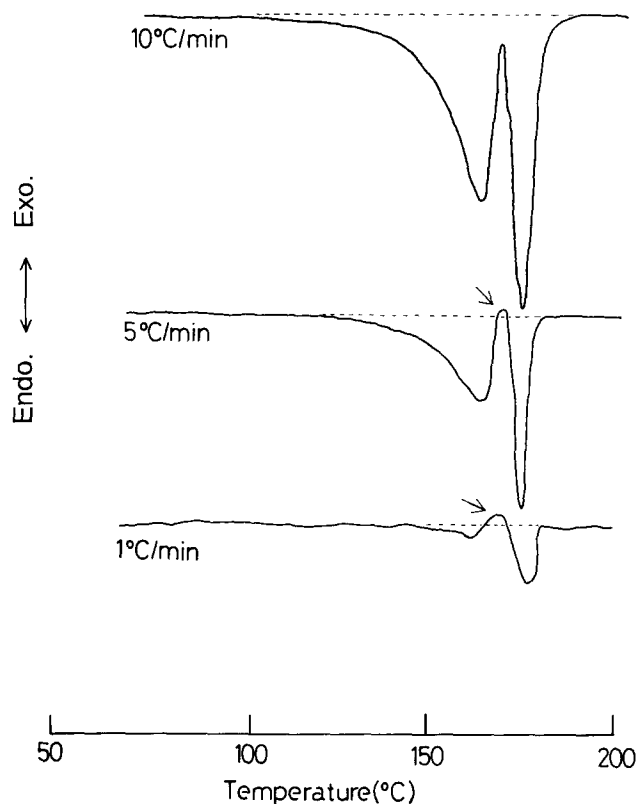


Figure 6 D.t.a. curves of the melt-quenched 80/20 PVDF/PMMA blends at various heating rates

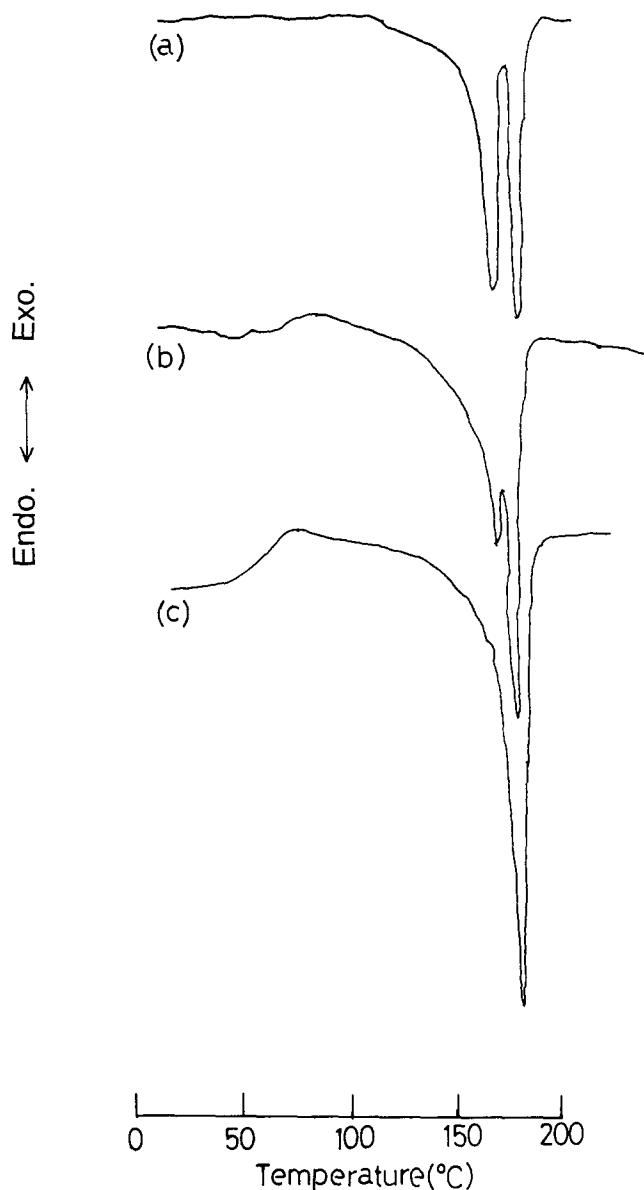


Figure 7 Remeasured d.t.a. profiles for the samples heated up to (a)  $157^{\circ}\text{C}$ , (b)  $163^{\circ}\text{C}$  and (c)  $167^{\circ}\text{C}$  and then melt quenched

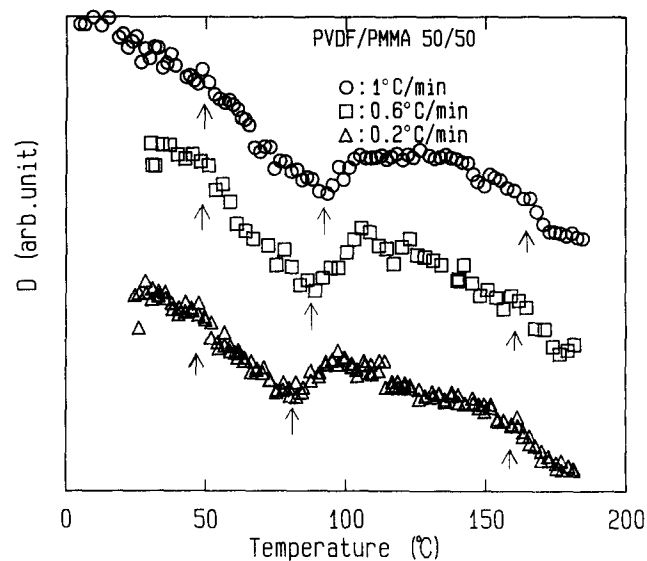


Figure 8 Temperature dependence of  $D$  measured at various heating rates

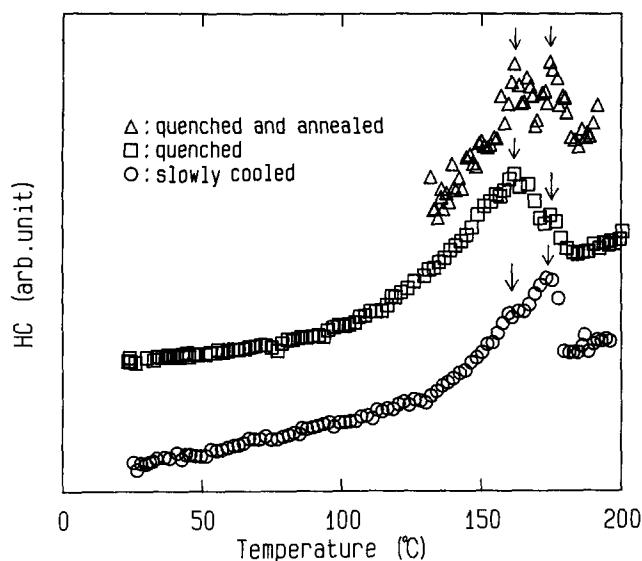


Figure 9 Temperature dependence of HC

exothermic peak due to cold crystallization at 100°C, and the X-ray diffraction pattern of the sample heated up to 100°C at a heating rate of 1°C min<sup>-1</sup> exhibited the growth of crystallization of the  $\alpha$  phase. Thus this increase of  $D$  is considered to be due to the crystallization of the PVDF component in the blend during heating.

#### Temperature dependence of HC

The temperature dependence of HC is shown for the 80/20 PVDF/PMMA samples prepared by melt quenching only, slow cooling only, and melt quenching and subsequent annealing at 120°C for 24 h in Figure 9. The heating rate is 1°C min<sup>-1</sup> for the melt-quenched and the slowly cooled samples and 0.2°C min<sup>-1</sup> for the melt-quenched and annealed one. The melt-quenched sample has a clear peak at 161°C and a shoulder at 173°C; the slowly cooled one has a shoulder at 161°C and a clear peak at 173°C; and the melt-quenched and annealed one has peaks at 162 and 175°C. The lower peak and shoulder in the vicinity of 160°C may be attributed to the onset of melting of the  $\beta$  crystal phase, corresponding to  $T'_m$  in the d.t.a. curve. The higher peak and shoulder at 173 or 175°C is ascribed to the onset of melting of the  $\alpha$  crystal phase, corresponding to  $T_m$  in the d.t.a. curve.

HC measurement of the sample prepared by melt quenching and subsequent annealing exhibits distinct

peaks due to the onset of melting of the  $\beta$  and  $\alpha$  crystal phases. It is noted that the temperature profile of HC gave information on the melting transition of the  $\beta$  and  $\alpha$  crystal phases, whereas that of  $D$  only shows the melting of the  $\alpha$  crystal phase.

#### CONCLUSION

The thermal diffusivity and the relative heat capacity of PVDF/PMMA blends were studied. The melt-quenched sample had a peak in  $D$  at PVDF/PMMA blend ratios of 75/25 and 80/20, although the X-ray diffraction patterns exhibited only a monotonic decrease of the crystallinity with decrease of PVDF content. We do not have a definite interpretation for this specific change of  $D$ , but can only say that this specifically larger  $D$  is related to some change of supermolecular structure. In other words, flash radiometry is a unique technique to catch a change of supermolecular structure that cannot be detected by the usual X-ray and thermal analyses. Furthermore, the temperature profiles of  $D$  and HC exhibit the glass transition as well as the melting transition of the  $\alpha$  and  $\beta$  crystal phases, which were consistent with the results of the thermal analysis.

#### ACKNOWLEDGEMENTS

The authors are sincerely grateful to Mr H. Horibe, Materials and Electronic Devices Laboratory, Mitsubishi Electric Co., Japan, for preparing blend samples.

#### REFERENCES

- 1 Tsutsumi, N. and Kiyotsukuri, T. *Appl. Phys. Lett.* 1988, **52**, 442
- 2 Tsutsumi, N., Takizawa, T. and Kiyotsukuri, T. *Polym. Commun.* 1988, **29**, 28
- 3 Tsutsumi, N., Takizawa, T. and Kiyotsukuri, T. *Polymer* 1990, **31**, 1925
- 4 Tsutsumi, N., Takeuchi, N. and Kiyotsukuri, T. *J. Polym. Sci. (B) Polym. Phys.* 1991, **29**, 1085
- 5 Tam, A. C. and Sullivan, B. *Appl. Phys. Lett.* 1983, **43**, 333
- 6 Leung, W. P. and Tam, A. C. *Opt. Lett.* 1984, **9**, 93
- 7 Leung, W. P. and Tam, A. C. *J. Appl. Phys.* 1984, **56**, 153
- 8 Choy, C. L., Leung, W. P. and Ng, Y. K. *J. Polym. Sci. (B) Polym. Phys.* 1987, **25**, 1779
- 9 Nishi, T. and Wang, T. T. *Macromolecules* 1975, **8**, 909
- 10 Leonard, C., Harlary, J. L., Monnerie, L., Broussoux, D., Servet, B. and Micheron, F. *Polym. Commun.* 1983, **24**, 110
- 11 Horibe, H., Baba, F. and Etoh, S. *Polym. Prepr. Japan* 1989, **38**, 3533
- 12 Agari, Y., Ueda, A., Nishioka, N. and Kosai, K. *Polym. Prepr. Japan* 1991, **40**, 1212
- 13 Hirata, Y. and Kotaka, T. *Polym. J.* 1981, **13**, 273